

# Overstrength factors of RC bridges supported on single and multi-column RC piers in Mexico

Alma R. Sánchez<sup>1</sup> | António Arêde<sup>2</sup>  | Jose M. Jara<sup>1</sup>  | Pedro Delgado<sup>2,3</sup> 

<sup>1</sup> School of Civil Engineering, University of Michoacan, Morelia, Mexico

<sup>2</sup> CONSTRUCT-LESE, Faculty of Engineering (FEUP), University of Porto, Porto, Portugal

<sup>3</sup> proMetheus, Instituto Politécnico de Viana do Castelo Rua Escola Industrial e Comercial Nun'Álvares, Viana do Castelo, Portugal

## Correspondence

José M. Jara, School of Civil Engineering, Universidad Michoacana de San Nicolás de Hidalgo, Santiago Tapia 403, Morelia 58000, Michoacán, México.

Email: [jmjara70@gmail.com](mailto:jmjara70@gmail.com)

## Funding information

FEDER funds, Grant/Award Number: POCI-01-0145-FEDER-007457; FCT/MCTES, Grant/Award Number: UID/05975/2020

## Abstract

Mexico highway network has more than 14,000 bridges. Most of them are reinforced concrete (RC) structures. The bridges design process incorporates the use of an overstrength factor that is not justified and has received little attention in published works. Mexican regulations allow using an overstrength factor for buildings in the range of 2–3, to reduce the design spectra as a function of the selected seismic behavior factor. However, for bridges, a single factor of 1.5 is proposed independent of any design parameter. The bridges in Mexico are mostly simply supported structures with maximum span lengths of 50 m. A relevant and distinctive aspect of the bridges designed in Mexico is the large load amplitudes of the trucks used to define the live load and the high seismic activity in the country. This study determines overstrength factors of a family of medium-length RC bridges composed of simply supported superstructures and substructure made up of single and multi-column RC piers. Non-linear dynamic analyzes using a set of 80 accelerograms were carried out. The results show that the height of the bridges and their seismic location are relevant parameters in the overstrength of the structures. Finally, analytical expressions are proposed to assess the overstrength factors of a very common bridge typology in Mexico and the world.

## KEYWORDS

effect of pier height on overstrength factors, empirical equations to obtain overstrength factors in rc bridges, influence of the type of substructure on overstrength factors, nonlinear dynamic analysis of RC bridges

## 1 | INTRODUCTION

Bridges are essential structures for the economic development of a country. During an earthquake occurrence, it is important to limit damages in bridges to reduce the economic impact of the event. Despite the great seismic activity in Mexico, bridge design regulations in Mexico are scarce and the generation of bridge standards follows a much slower process than the standards for other structures as buildings.

The national highway network in Mexico included, at the end of 2014, 16,656 bridges (8493 in toll-free roads and 8163 in toll roads) located mostly in highly seismic or intermediate seismic areas.<sup>1</sup> About 31% of the structures are in areas of high seismicity and 29% in areas of intermediate seismicity.

Bridge regulations recognize that the real strength of the structures when subjected to lateral loads beyond the material yielding, is greater than the nominal design strength, due to various factors that include the design methodology, the

strength increase of the reinforcement bars in the zone of strain hardening, the increase of concrete strength over time, the cross-sectional dimensions of the structural elements and the provided steel area that is normally greater than required, among others.

For decades, the importance of overstrength in the seismic response of structures has been recognized, which sometimes explains observed seismic damages.<sup>2</sup> Other authors<sup>3–8</sup> have suggested that other possible sources of overstrength in structures are: overdesign for gravitational loads, slab contribution to the resistance of beams with negative moments, the participation of non-structural elements, the minimum strength requirements established in the regulations, the contribution of compressive steel in elements subjected to bending, the strength increase for short-term loads, the structural redundancy, the use of the elastic period in the design process and the load-velocity relationship.

Overstrength factors of buildings have been reported with a significant range of variability. Miranda and Bertero<sup>9</sup> studied buildings in Mexico City and found overstrength factors in the range of 2–5 and mentioned the importance of infill masonry walls and the slab contribution to overstrength. For steel buildings, Osteraas and Krawinkler<sup>10</sup> reported overstrength factors in the range of 1.8–6.5 in buildings designed in accordance with the UBC code.<sup>11</sup> Shahrooz and Moehle<sup>12</sup> experimentally studied a 1:4 scale model of a structure formed by six-story reinforced concrete frames and found an overstrength value of 7.65.

Cassis and Bonelli<sup>13</sup> reported overstrength factors in the range of 3–5 for reinforced concrete frames, walls and frame-wall systems. The authors concluded that the overstrength factors in the frame systems were greater than those of the other two cases analyzed. Zhu et al.<sup>14</sup> found that the overstrength is greater for low-rise buildings compared to higher-rise buildings. Jain and Navin<sup>15</sup> coincide with this conclusion based on the study of three-story and nine-story buildings. They found an important dependence of overstrength with the seismic zone where the buildings were located, among five different sites studied in India. The seismic location of the structure was a very relevant parameter in overstrength factors. The average overstrength factors of the buildings located in the highest seismicity zone was of 2.8, whereas this value increased to 12.7 for the buildings located in the lowest seismicity zone.

In a study of ten-story braced frames,<sup>16</sup> the authors found overstrength factors in the range of 1.5–3.5. The authors suggested that one of the parameters that most influences the overstrength is the force redistribution when the structure enters into the inelastic range. Balendra and Huang<sup>17</sup> analyzed steel frames in the range of three-ten stories with three numerical models: moment-resisting frames, frames with concentric bracing and frames with semi-rigid connections. The frames designed to support gravitational load presented overstrength factors of 3.5 and 8.0 for ten- and three-story structures, respectively. These values were reduced by half when considering the semi-rigid connections and the overstrength of braced models was found in the range of 2.5–5.5. The influence of the dynamic properties of the buildings in the overstrength factors is also showed in the study of one- to ten-story buildings,<sup>18</sup> finding overstrength factors in the range of 5.5–2.1.

Ghee et al.<sup>19</sup> tested a set of 25 RC circular columns for bridges. The influence of axial load, transverse reinforcement, and flexural ductility on overstrength was evaluated. Depending on the level of axial load, the overstrength factor was found in the range of 1.0–2.3.

Kappos et al.<sup>20</sup> studied seven bridges located in an area of high seismicity in Europe. They considered in the analysis continuous bridges and simply supported bridges on elastomeric bearings. The overstrength factor was obtained with pushover analyses as the ultimate shear force to design shear force ratio. The authors found overstrength factors in the range of 1.3–3.4 in the longitudinal direction of the bridges and in the range of 1.2–5.8 in the transverse direction.

In Mexico, there is a lack of studies that quantify the overstrength in bridges considering the seismic sources of the country and particularly assessing the influence of bridge typologies. The current version of the Civil Works Design Manual of the Federal Electricity Commission,<sup>21</sup> in its chapter of Earthquake Design, specifies an overstrength factor of 1.5 to reduce the design spectra used for designing bridges. However, this factor is adopted without any proper justification. Conversely, the Civil Works Design Manual<sup>21</sup> describes in detail the overstrength factors established for building design. However, the differences between the support system and redundancy in buildings and bridges suggest that overstrength factors for bridges should be assessed.

Bridges in Mexico are designed for trucks weight up to 72.5 t, a value considerably higher than that used for the design of bridges in many countries worldwide. Additionally, the seismic hazard of most of the Mexican Republic is governed by interplate and intraplate seismic sources. These seismic faults have the potential to generate events of  $M > 8$  and control the design of bridges located in central and southern Mexico. The similar contribution of these two seismic sources in the seismic hazard in many regions, the methodology used to assess the seismic hazard and the large amplitude of the design live loads, make bridges in Mexico particularly different from other sites. In Mexico, load combinations of the AASHTO standards of the United States are used. However, the bridges designed in both nations are considerably different mainly

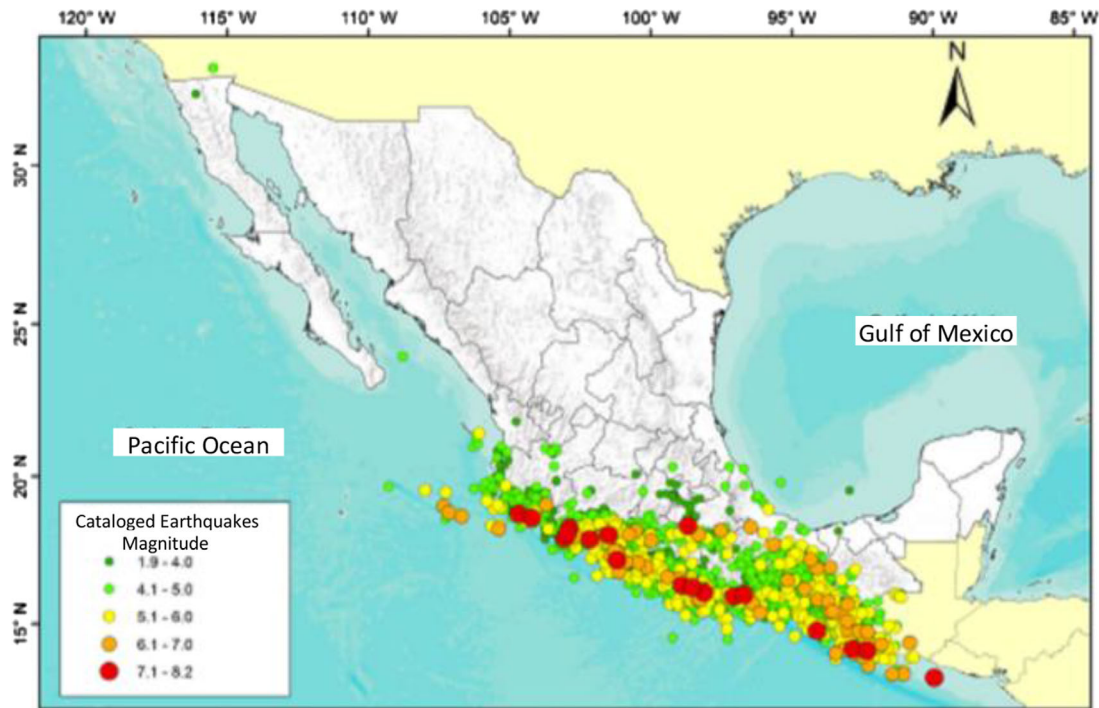


FIGURE 1 Earthquake epicenters in Mexico recorded in the period of 1964 to 2017<sup>22</sup>

due to: (1) the seismic hazard in the United States is fundamentally governed by a single seismic source (transcurrent fault), whereas in Mexico, interplate and intraplate seismic sources similarly contribute to the seismic hazard; (2) in the United States the return period used for design bridges is 1000 years; in Mexico, the seismic code establishes optimal design spectra that have variable return periods as a function of the seismic hazard in the country, and (3) the weight of design trucks are considerably different in both countries.

This study determines overstrength factors of medium-length RC bridges with common typologies composed of two extensively used substructures: frame-type substructure and single column piers. The overstrength factor is defined as the ratio of ultimate base shear to design base shear. Nonlinear dynamic analyses of the bridges subjected to a set of 80 seismic records were carried out. The analyses include two types of superstructure, two types of substructure, four pier heights and three seismicity zones. The lack of specific studies in Mexico to assess overstrength factors in bridges and the high amplitude of live loads used to design bridges in the country motivated the study. As a result, numerical expressions are proposed to obtain the overstrength factors of medium-length RC bridges supported on single column and multi-column RC piers.

## 2 | SEISMIC DEMAND

Seismic records were collected from two seismic sources that have produced structural damages in the seismic history of Mexico. One of them is an interplate seismic source that generates very frequently strong earthquakes with epicenters located close to the Mexican Pacific Coast. The second seismic source is an intraplate seismic source that generates earthquakes with hypocentral depths greater than 45 km and normally the epicenters are inside the continent. Both seismic sources, with independent occurrence processes, have the potentiality of generating earthquakes with magnitude  $M_w > 8$ , although the frequency of occurrence is higher in the interplate seismic source.

Figure 1 shows a map of earthquake epicenters in Mexico recorded in the period from 1964 to 2017. Mexico has several seismic sources, namely: a transcurrent fault in the north of the country, interplate faults in the south-west, intraplate faults in the central and south-west region and local faults in central area. Interplate earthquakes are produced by the subduction of the Rivera and Cocos plates under the North American plate. The epicenters are in the Pacific Coast between Chiapas and Jalisco states. The epicenters inside the continent are produced in local and intraplate faults. Whereas

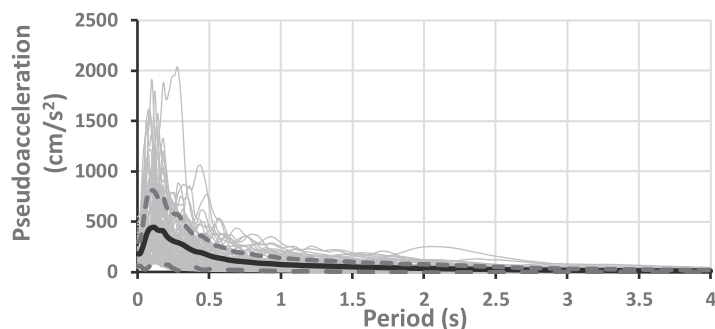


**FIGURE 2** Response spectra for 5% of critical damping. Mean spectrum is in solid black line and dashed lines are mean spectrum  $\pm$  one standard deviation



**FIGURE 3** (A) Multi-column and (B) single column bridges in Mexico

hypocentral depths of interplate tremors are usually in the range of 10–45 km, intraplate hypocentral depths are greater than 45 km.

A set of 80 seismic records from both seismic sources were selected. All accelerograms were recorded in seismic stations located on hard soil sites, defined as those soils with shear wave velocities  $V_s$  greater than 720 m/s. The selection criteria, in addition to the type of soil, considered those seismic records with the highest spectral amplitudes.

Figure 2 shows the response spectra of the family of seismic records for 5% of critical damping. The figure also shows the mean spectrum and the mean  $\pm$  one standard deviation. Maximum spectral amplitudes are located in the period's zone below 0.5 s, because seismic stations are in sites of hard soil. The scaling process of the accelerograms was based on the acceleration spectrum intensity (ASI)<sup>23</sup> in the period range of 0.1–0.5 s. The ASI of uniform hazard spectra for different return periods was determined at the bridge location sites. The uniform hazard spectra were obtained from the most recent seismic hazard study conducted in Mexico.<sup>21</sup> All seismic records were scaled with the factor obtained by dividing the ASI value of the uniform hazard spectrum, for a specific return period, by the ASI value of each response spectrum of the accelerograms. The scaling of accelerograms followed an increase process of return periods until reaching the bridge failure, according to Section 4.

### 3 | NUMERICAL MODELS

Most of RC bridges in Mexico are composed of several simply supported spans with a maximum length span of 50 meters.<sup>24</sup> The numerical models for this study are five-span simply supported bridges on elastomeric bearings. Two span lengths are included: 30 and 50 m. In the first case, a superstructure composed of AASHTO type IV girders is used and in the second case Nebraska type 240 girders are used. In both cases, the bridge deck is a 0.20 m thick RC slab. The most common substructures in the country are composed of single (Figure 3B) and multi-column piers (Figure 3A), forming in the latter case a frame-type substructure in the transverse direction.

Two RC substructure types are analyzed: single column piers (Figure 4B) and piers formed with four columns (Figure 4A). The pier height was also a variable considered in the analysis, varying this parameter in the range of 5–20 m, at increments of 5 m. Finally, the bridges were designed in three different seismic locations, namely: low (LS), medium (MS)



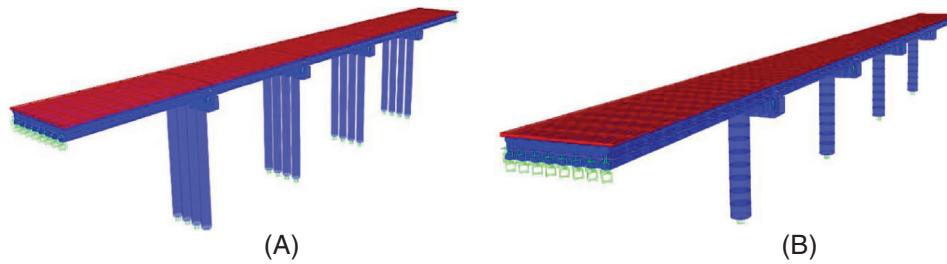


FIGURE 4 Numerical models of bridges. (A) Multi-column piers and (B) single column piers

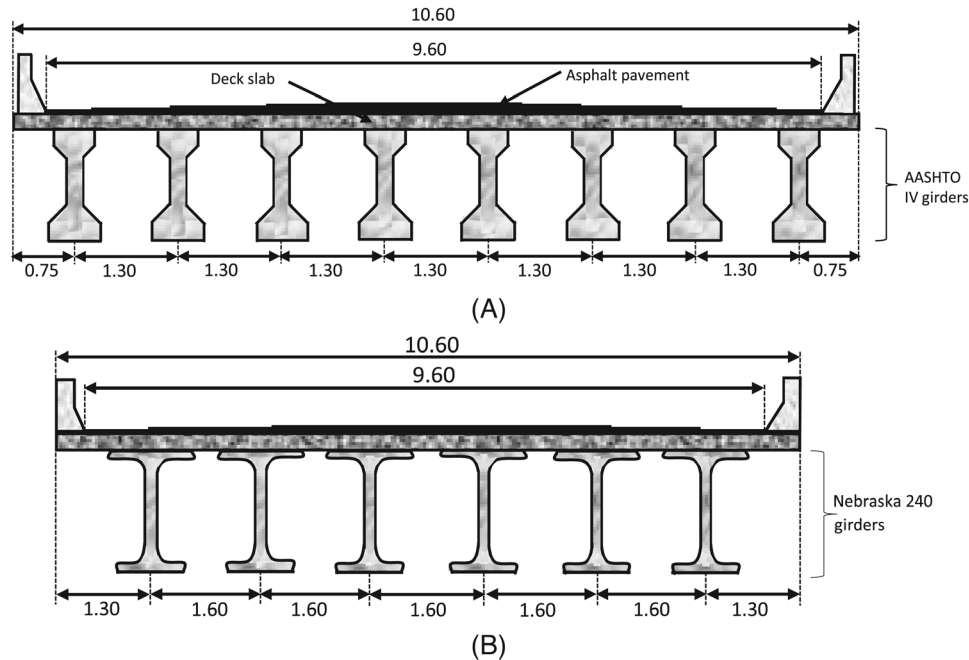


FIGURE 5 Bridges cross section. (A) AASHTO IV girders for 30 m span bridges and (B) Nebraska 240 girders for 50 m span bridges

and high seismicity (HS). The parameter combination leads to a total of 48 numerical models that were subjected to the set of 80 seismic records.

RC deck slab has a weight density of  $23.5 \text{ kN/m}^3$  and the thickness of asphalt pavement for the bridges design was of 0.10 m, with a weight density of  $21.6 \text{ kN/m}^3$ . The overall width of the bridges is 10.60 m (two-lane road) with a roadway width of 9.60 m (Figure 5). In the transverse direction, the bridges have RC rectangular cross beams with a constant width of 0.30 m. The separation of cross beams is  $1/6 L$  for the 30 m spans (Figure 5A) and  $1/10 L$  for the 50 m spans (Figure 5B). The beams rest on elastomeric bearings designed for each case of analysis.

Figure 6 shows the numerical model of one of the five span bridges. The RC slab was modeled with shell-type finite elements (quadrilateral elements with six degrees of freedom at each joint). The beams and columns were modeled with bar-type elements with six degrees of freedom at each node. The columns were discretized into various elements to consider their mass along their length. The elastomeric bearings were modeled with link-type linear elements of two nodes and six degrees of freedom at each node. The model of expansion joints is a gap type non-linear link element that considers a possible gap closure in the longitudinal direction.

The interaction between backfill and abutments was modeled according to the recommendations established in Caltrans.<sup>25</sup> In the longitudinal direction, a bilinear model was used. The initial embankment fill stiffness for the case of a fill not meeting the requirements of the Standard Specifications was used ( $K_i = 14.35 \text{ kN/mm/m}$ ). The bridges have seat-type abutments and according to the backwall width and bridge height, the effective abutment wall stiffness was determined.

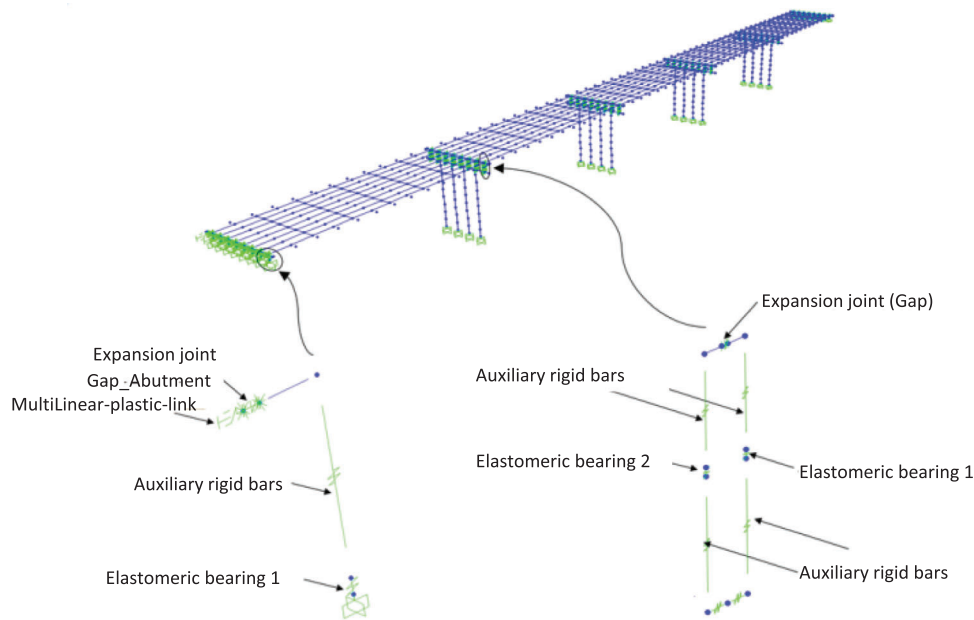


FIGURE 6 Detailed numerical model of the five span bridges

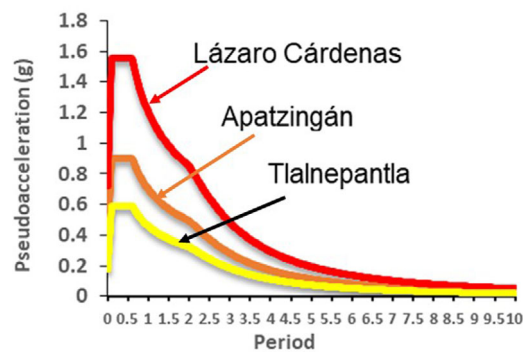


FIGURE 7 Design spectra for low seismicity zone (Tlalnepantla), medium seismicity zone (Apatzingán) and high seismicity zone (Lázaro Cárdenas)

Deck slab, kerbs, cross beams, bent caps, and columns were RC elements with compressive strength  $f'_c = 24.5$  MPa. Compressive strength in girders were  $f'_c = 34.3$  MPa and  $f'_c = 44.1$  MPa for AASHTO IV and Nebraska beams, respectively. The modulus of elasticity of concrete was  $E_c = 4400(f'_c)^{1/2}$  ( $f'_c$  in MPa), the modulus of elasticity of steel was  $E_s = 205940$  MPa and the yield strength of the reinforcing steel was  $f_y = 412$  MPa.

The bridges were located on hard soil sites in three seismic zones, namely: low, medium, and high seismicity. The soil-structure interaction was neglected and fixed column supports were assigned. Figure 7 shows the design spectra of the three places. In all cases, the plateau of the spectra starts at a period of  $T_i = 0.1$  and finishes at  $T_f = 0.6$  (hard soil sites). The maximum spectral amplitudes are in the range of 0.6–1.56 g, from low to high seismicity zones. A seismic behavior factor  $Q = 2.0$  was adopted to design the bridges carried out with SAP2000 program.<sup>26</sup> The load combinations for Strength I and Extreme Event I limit states included in the AASHTO standards<sup>27</sup> were used in the design process.

Figure 8 shows the trucks used to design the bridges. According to the requirements established in two lane bridges, an HS-20 truck (Figure 8A) must be used in one design lane combined with a truck in the other lane of the most unfavorable condition of trucks T3-S3 (Figure 8B) or T3-S2-R4 (Figure 8C).

The design of the structural elements was carried out based on the Complementary Technical Standards for the Design and Construction of Concrete Structures of the Mexico City Building Code<sup>28</sup> using the load combinations of the AASHTO standards.<sup>27</sup> Mexico City code is a force-based standard that establishes, for structural analysis, the use of cracked moments of inertia of 0.5I g for beams and 0.7I g for columns, where I<sub>g</sub> is the moment of inertia of the concrete gross cross-section.

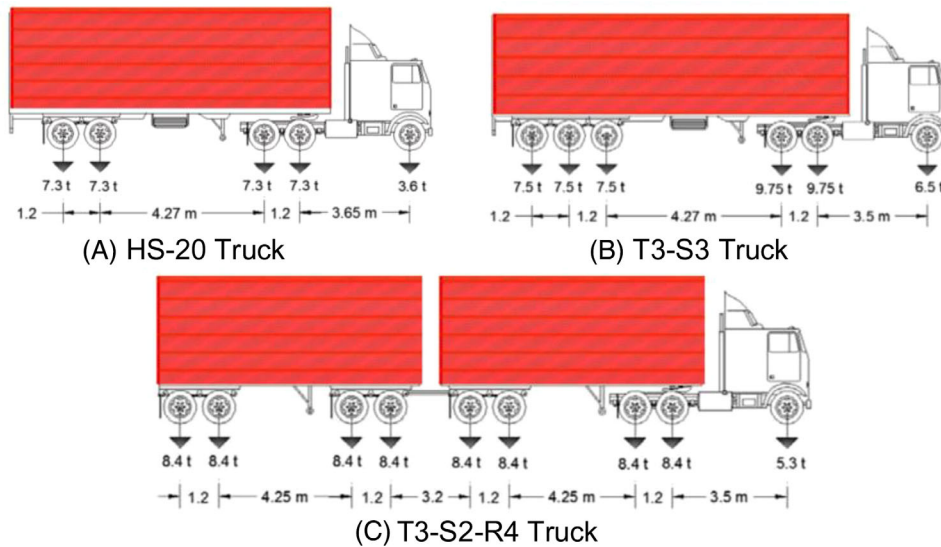


FIGURE 8 Trucks loadings used for designing the bridges

The reinforcement ratio of longitudinal steel in columns is limited in the range of 1% to 6% and 1% to 4% for structures designed with  $Q = 2$  and  $Q = 4$ , respectively, where  $Q$  is the seismic behavior factor. For the design of the bridges in this study ( $Q = 2$ ), the code specifies a minimum diameter of 7.9 mm for transverse reinforcement. In spiral reinforcement, the minimum volumetric ratio of transverse reinforcement is 0.0071. The cross-section height/width ratio in beams should not exceed six and in columns this limit is four. For  $Q = 2$ , the code also establishes that  $\Sigma M_e \geq \Sigma M_g$ , where  $M_e$  is the sum of resistant moments of the columns that reach the node and  $M_g$  is the sum of resistant moments of the beams reaching the node, thus corresponding to adoption of capacity design method. The design criteria change as a function of the seismic behavior factor selected for the design ( $Q = 2, 3, \text{ or } 4$ ), but they are independent of the seismic zone.

Table 1 shows column dimensions and steel ratios of each bridge model. It is also included the nomenclature used to identify the numerical models. The first character, M or C, identifies the substructure type (M = multi-column pier and C = single column pier). The next two characters refer to the span length, followed from the pier height (xx) Pxx and finally the last number displays the bridge location (1 = low seismicity; 2 = medium seismicity and 3 = high seismicity). Multi-column bridges with span length of 30 m have circular columns with diameter in the range of 0.90–1.80 m and this range is of 0.95–1.85 m for 50 m span bridges. Steel ratios are in the range of 2.85% to 3.16%. Conversely, column diameters in single column bridges are in the range of 1.60–3.10 m and 1.70–3.20 m for span lengths of 30 m and 50 m, respectively. Steel ratios in these cases are in the range of 2.82% to 3.13%.

The maximum axial load ratio ( $P_{max}/A f'_c$ ) in columns varied in the range of 0.06–0.23.  $P_{max}$  is the maximum axial load of all design combinations. The transverse reinforcement consisted of stirrups No. 4 ( $A_s = 127 \text{ mm}^2$ ) and No. 5 ( $A_s = 198 \text{ mm}^2$ ). The stirrups spacing in columns was in the range of 90–130 mm and 60–130 mm for the 30 m span and 50 m span bridges, respectively.

Table 2 shows the fundamental periods of the bridges in both directions of analysis. Bridges' periods with multi-column substructure were in the range of 0.89–3.28 s in the longitudinal direction and in the range of 0.83–2.35 in the transverse direction. Bridges supported on single column substructures had fundamental periods in the range of 0.85–3.29 s in the longitudinal direction and in the range of 0.90–3.81 s in the transverse direction. All fundamental periods are in the descending zone of the design spectra. The plateau region ends at a period of  $T_s = 0.6 \text{ s}$  for sites of hard ground.

The girders of most of the short and medium length bridges in Mexico rest on elastomeric bearings. The design of the bearings follows the procedure described in AAHSTO regulation code<sup>27</sup> that limits shear strain demands under dead and live loads' action. They are composed of layers of Shore A-60 Neoprene (Chloroprene Rubber) and steel plates. The bearing dimensions (in millimeters) in this study were in the  $300 \times 300 \times 41$ – $400 \times 400 \times 185$  range (length  $\times$  width  $\times$  thickness), and the shear modulus was  $G = 1.0 \text{ MPa}$ . In service conditions, shear deformations were limited to 50% of the elastomer thickness to avoid delamination due to fatigue. The bearings lateral stiffness was in the range 1.07 to 2.0 kN/mm, whereas the vertical stiffness ranged from 324 to 510 kN/mm. The bearings/pier lateral stiffness ratio varied from 0.05 to 15.0. Displacement capacity of this type of bearings corresponds to shear strain of 200%, which for the models' bearing

TABLE 1 Bridge characteristics of the numerical models

Span length (m)	Pier height (m)	Seismic zone	D (m)	Steel ratio (%)	Pmax/A f'c	Model ID	Span length (m)	Pier height (m)	Seismic zone	D (m)	Steel ratio (%)	Pmax/A f'c	Model ID
30	5	Low	0.90	2.85	0.19	M30P05-1	50	5	Low	0.95	3.19	0.23	M50P05-1
		Medium	1.05	2.85	0.17	M30P05-2			Medium	1.10	2.88	0.21	M50P05-2
		High	1.25	3.00	0.16	M30P05-3			High	1.30	2.83	0.19	M50P05-3
	10	Low	0.95	3.22	0.18	M30P10-1		10	Low	1.05	2.88	0.22	M50P10-1
		Medium	1.15	2.98	0.17	M30P10-2			Medium	1.25	3.16	0.20	M50P10-2
		High	1.50	3.02	0.17	M30P10-3			High	1.55	2.99	0.18	M50P10-3
	15	Low	1.12	2.90	0.15	M30P15-1		15	Low	1.18	2.99	0.20	M50P15-1
		Medium	1.25	3.05	0.14	M30P15-2			Medium	1.30	3.24	0.18	M50P15-2
		High	1.65	3.05	0.14	M30P15-3			High	1.75	2.95	0.16	M50P15-3
	20	Low	1.30	2.91	0.13	M30P20-1		20	Low	1.35	2.90	0.16	M50P20-1
		Medium	1.45	2.91	0.13	M30P20-2			Medium	1.50	2.91	0.15	M50P20-2
		High	1.80	2.93	0.13	M30P20-3			High	1.85	3.01	0.14	M50P20-3
30	5	Low	1.60	2.84	0.16	C30P05-1	50	5	Low	1.70	2.92	0.22	C50P05-1
		Medium	1.80	2.84	0.14	C30P05-2			Medium	1.90	2.83	0.19	C50P05-2
		High	2.05	3.13	0.10	C30P05-3			High	2.20	2.85	0.14	C50P05-3
	10	Low	1.75	3.07	0.16	C30P10-1		10	Low	1.90	2.97	0.19	C50P10-1
		Medium	2.10	2.83	0.15	C30P10-2			Medium	2.20	2.82	0.16	C50P10-2
		High	2.50	2.95	0.11	C30P10-3			High	2.55	2.99	0.15	C50P10-3
	15	Low	1.90	2.94	0.15	C30P15-1		15	Low	2.00	2.86	0.19	C50P15-1
		Medium	2.25	3.01	0.13	C30P15-2			Medium	2.35	2.98	0.16	C50P15-2
		High	2.80	3.05	0.09	C30P15-3			High	2.90	2.88	0.11	C50P15-3
	20	Low	1.75	2.96	0.15	C30P20-1		20	Low	1.90	2.83	0.19	C50P20-1
		Medium	2.40	3.05	0.12	C30P20-2			Medium	2.40	3.05	0.15	C50P20-2
		High	3.10	2.97	0.06	C30P20-3			High	3.20	2.79	0.08	C50P20-3

dimensions, led to displacement capacities in the range 82–370 mm. For bridges with span length of 30 m, neoprene JCMY-55 expansion joints with 40 mm gap width of were used, whereas for 50 m long span bridges neoprene MT-50 expansion joints were adopted with 80 mm gap width.

#### 4 | NONLINEAR ANALYSIS

To quantify the overstrength, the ultimate capacity of the bridges was determined based on non-linear analysis of the bridges subjected to the family of the seismic records. Ultimate capacity was assumed when the element reached one or more of the following conditions: (a) a drop of 20% of the moment capacity; (b) a tension strain demand in the longitudinal steel equal to its maximum strain capacity, and (c) a compression strain demand in concrete equal to its maximum strain capacity. Fiber response was obtained from the nonlinear constitutive models of the reinforcing steel and concrete. The overstrength factor was determined as the ratio of the ultimate base shear capacity to the design base shear. The nonlinear models were created using the SAP2000 program<sup>26</sup> with viscous damping of 1%, assuming that the nonlinear behavior occurs in piers and using a fiber-type section model.

Fiber P-M2-M3 hinges were assigned and the program SAP2000 integrates the axial behavior of the fibers to get moment rotation curves. Figure 9 shows a cross section of the column discretized into the number of integration points. Each fiber is described with a uniaxial constitutive relationship in the zone of plastic behavior at both column ends. The number of fibers used to discretize the cross section was in the range of 526–2523, as a function of the column diameter and the longitudinal steel distribution.



TABLE 2 Fundamental periods of the bridges

Model ID	T <sub>long</sub> (s)	T <sub>tran</sub> (s)	Model ID	T <sub>long</sub> (s)	T <sub>tran</sub> (s)	Model ID	T <sub>long</sub> (s)	T <sub>tran</sub> (s)	Model ID	T <sub>long</sub> (s)	T <sub>tran</sub> (s)
M30P05-1	1.12	0.87	M50P05-1	2.06	1.88	C30P05-1	0.94	1.04	C50P05-1	1.92	2.01
M30P05-2	0.99	0.85	M50P05-2	1.96	1.86	C30P05-2	0.89	0.96	C50P05-2	1.89	1.95
M30P05-3	0.89	0.83	M50P05-3	1.89	1.85	C30P05-3	0.85	0.90	C50P05-3	1.86	1.90
M30P10-1	1.67	1.13	M50P10-1	2.58	2.03	C30P10-1	1.27	1.46	C50P10-1	2.16	2.30
M30P10-2	1.37	0.97	M50P10-2	2.26	1.94	C30P10-2	1.07	1.17	C50P10-2	2.02	2.11
M30P10-3	1.05	0.88	M50P10-3	2.02	1.89	C30P10-3	0.94	1.00	C50P10-3	1.93	1.99
M30P15-1	1.89	1.33	M50P15-1	3.03	2.21	C30P15-1	1.58	1.91	C50P15-1	2.55	2.78
M30P15-2	1.70	1.17	M50P15-2	2.75	2.10	C30P15-2	1.32	1.49	C50P15-2	2.25	2.38
M30P15-3	1.27	0.95	M50P15-3	2.18	1.93	C30P15-3	1.06	1.14	C50P15-3	2.02	2.09
M30P20-1	2.04	1.52	M50P20-1	3.28	2.35	C30P20-1	2.08	3.02	C50P20-1	3.29	3.81
M30P20-2	1.84	1.30	M50P20-2	2.94	2.19	C30P20-2	1.55	1.82	C50P20-2	2.60	2.82
M30P20-3	1.47	1.05	M50P20-3	2.42	2.00	C30P20-3	1.18	1.28	C50P20-3	2.11	2.19

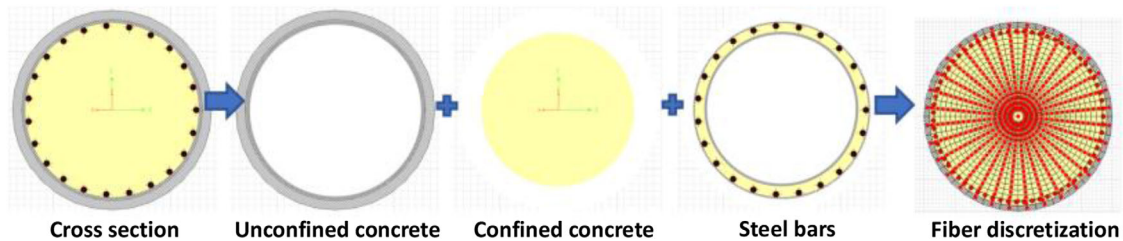


FIGURE 9 Fiber discretization of the column cross section

The uniaxial constitutive model of concrete was based on the proposal of Mander et al.<sup>29</sup> For the reinforcing steel, Park and Paulay<sup>30</sup> constitutive model was adopted. Figure 10 shows the material constitutive models used for unconfined concrete (Figure 10A) and for reinforcing steel (Figure 10B). Equation 1 defines the plastic hinge length.<sup>31</sup>

$$L_p = 0.08L_c + 0.022f_y d_b \geq 0.044f_y d_b \quad (1)$$

$L_p$  is the plastic hinge length,  $L_c$  is the column length,  $d_b$  is the diameter of the longitudinal reinforcing bars, all of them in meters, and  $f_y$  is the yield strength of longitudinal steel in MPa.

According to figure 10, the yield and ultimate strain of the reinforcing steel was 0.002 and 0.108, respectively. The ultimate strain of the unconfined reinforced concrete was 0.005. The ultimate strain of the confined concrete, which depends on the geometric properties and the longitudinal and transverse reinforcements of each column, was in the range 0.018–0.026.

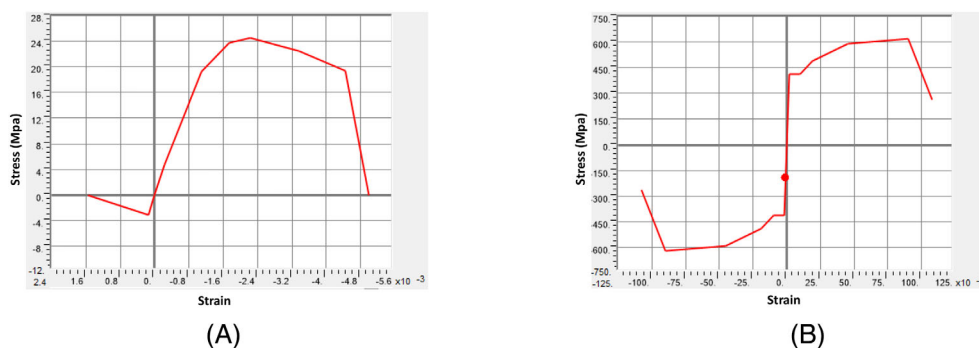


FIGURE 10 Uniaxial constitutive models. (A) Unconfined concrete and (B) reinforcement steel

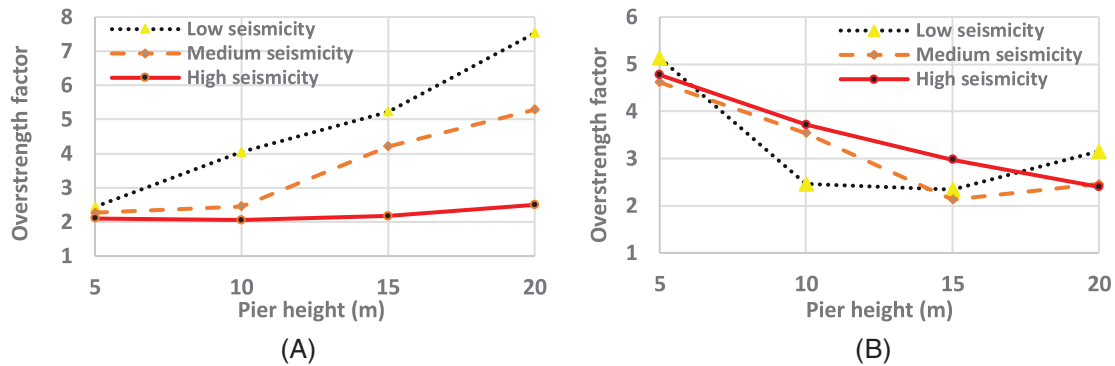


FIGURE 11 Overstrength factors of 30 m span bridges with multi-column piers. (A) Longitudinal direction and (B) transverse direction

The volumetric transverse reinforcement ratio of the columns in all models was the required to avoid a brittle failure in the piers. Moreover, at the end of the nonlinear analysis, shear demands were analyzed in all elements to verify that effectively piers failed in flexure before reaching a premature shear failure.

## 5 | OVERSTRENGTH FACTORS

The overstrength factor ( $q_s$ ) was obtained in each direction of analysis of the bridges as the ratio of the ultimate base shear to the design base shear. The ultimate base shear was assessed by subjecting the bridges to the three components of the set of 80 seismic records and following the failure criteria mentioned in the previous section.

### 5.1 | Bridges with span length of 30 m

Figure 11 shows mean values of the overstrength factors (average of the 80 factors computed from each seismic record) in both directions of multi-column bridges with span length of 30 m. Figure 11A shows overstrength factors in the longitudinal direction. The horizontal axis displays pier heights and vertical axis presents the overstrength factors.

In the high seismicity zone, the pier height had little relevance in the overstrength factors that have values in the range of 2.1–2.5. On the contrary, the overstrength factors of the bridges located in the medium and low seismicity zones showed a clear dependence on the pier height; the higher the pier, the greater the overstrength factor. In the medium seismicity zone, the factors were in the range of 2.3–5.3 and in the low seismicity zone overstrength factors were in the range of 2.4–7.5. The bridges with tall piers showed important changes in the overstrength factors when moving from low to high seismicity zones.

The growth of the overstrength factor as a function of the pier height observed in the longitudinal direction for the low and medium seismicity zones is mainly attributable to the increase in the ultimate base shear between the 5 and 20 m high models. The low and moderate participation of seismic loads in the design actions of the bridges located in these zones, caused an important contribution of gravity loads in bridges' design that provided overstrength to the bridges. Additionally, as the bridge height grows the displacement demands rise as well, and the participation of the abutments in the overstrength factors for the longitudinal direction became evident. The low-height bridges had overstrength factors similar for the three seismic zones as a result of similar displacements demands and negligible participation of abutments. Conversely, in the high seismicity zone, the seismic actions had the greatest contribution in the design for all bridge heights, which caused that the overstrength factor remains at similar values in all cases. In this seismic zone, by reducing the importance of gravity loads in the design, the increase in the design base shear is similar to the increase in the ultimate base shear when the pier height increases.

In the transverse direction (Figure 11B), the increase of the pier height reduces the overstrength factor. The bridges in the high seismicity zone presented overstrength factors in the range of 2.4–4.8, in the medium seismicity zone in the range of 2.1–4.6 and in low seismicity zone in the range of 2.3–5.1. Although there are considerable differences among the overstrength factors in the low and high seismicity zones, these variations are smaller than those observed in the longitudinal direction. Clearly, the change of behavior is associated with the different pier deformed shapes in both translational

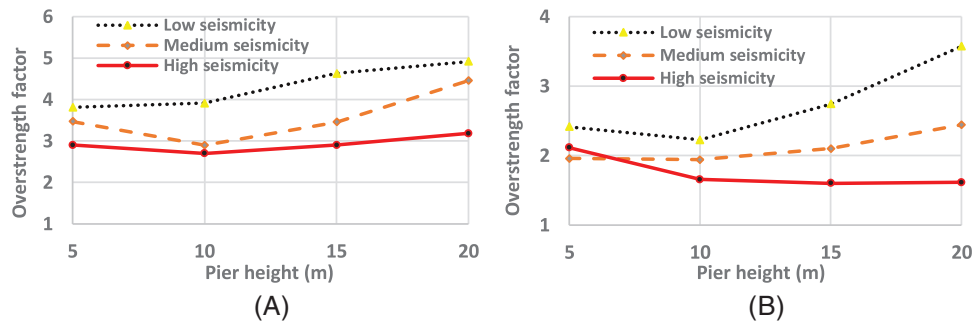


FIGURE 12 Overstrength factors of 30 m span bridges with substructure consisted of single column piers. (A) Longitudinal direction and (B) transverse direction

directions. Whereas in the longitudinal direction piers deform laterally in single curvature, they deform in double curvature in the transverse direction.

In the transverse direction, frame-type piers, formed by four columns and a cap beam, support the bridge. In this direction of analysis, similarly to the results published in previous studies,<sup>10,15</sup> the impact of the gravity loads on the design actions for low-height bridges originated high overstrength values that decreased as the bridge height increases because of the important contribution of seismic demands in the design actions. The important participation of gravity loads in the bridge overstrength factors, provides relevance to studies such as the one carried out here, particularly in view of the diversity of live loads used to design bridges in different countries. In frame-type piers, the collapse rotation demand of the 5 m high columns was reached in all cases for lateral displacements lower than those of the 20 m high bridges. The less stiffness of the 20 m high piers produced larger displacements that eventually caused to reach collapse damage state for lower shear forces than those of the 5 m high bridges.

Figure 12 shows the results of 30 m span bridges supported by single column piers. Figure 12A shows the overstrength factors for the longitudinal direction of the bridges and Figure 12B for the transverse direction. In the longitudinal direction, the rate of increase of overstrength factors observed in bridges supported on frame type piers and located in medium and low seismicity zones, is reduced when passing from short to tall piers in single column bridges.

In the high seismicity zone, both types of substructures displayed overstrength factors practically independent of the pier length. However, the overstrength was slightly higher in bridges supported on single column piers. In the longitudinal direction, the overstrength factors were in the range of 3.8–4.9, 2.9–4.5, and 2.7–3.2, for the low, medium, and high seismicity zones, respectively.

In the transverse direction, overstrength factors again decrease (up to certain height) and start increasing later (similar effect observed in bridges with four-column piers located in low and medium seismicity zones). The overstrength factors in the transverse direction were in the range of 2.2–3.6, 1.9–2.4, and 1.6–2.1, for the low, medium, and high seismicity zones, respectively. The bridges located in the zone of high seismicity showed overstrength factors that decrease with the pier height in the range of 5–15 m and subsequently presented a slight increase for bridge heights in the range of 15–20 m.

## 5.2 | Bridges with span length of 50 m

Figure 13 shows the overstrength factors for bridges with span length of 50 m supported on multi-column piers. Figure 13A presents the results in the longitudinal direction and Figure 13B in the transverse direction.

Although the trend of the overstrength factors in the longitudinal direction of the bridges (Figure 13A) is similar to that of the bridges with spans of 30 m, the overstrength factors are slightly higher for 50 m span bridges. In the low seismicity zone, the overstrength factors were in range of 2.2–8.7, in the medium seismicity zone in the range of 2.1–6.2 and in the high seismicity zone in the range of 1.7–2.8. The impact of the span length in the substructure design is smaller for short-pier bridges than tall-pier bridges, which is reflected in the overstrength factors.

In the transverse direction of the 50 m span bridges (Figure 13B), the overstrength factors showed a similar trend to that obtained for spans of 30 m. The overstrength factors were in the range of 2.4–4.5, 1.7–4.2, and 3.1–3.8 for the low, medium, and high seismicity zones, respectively. The major influence of the span length in overstrength factors was observed in

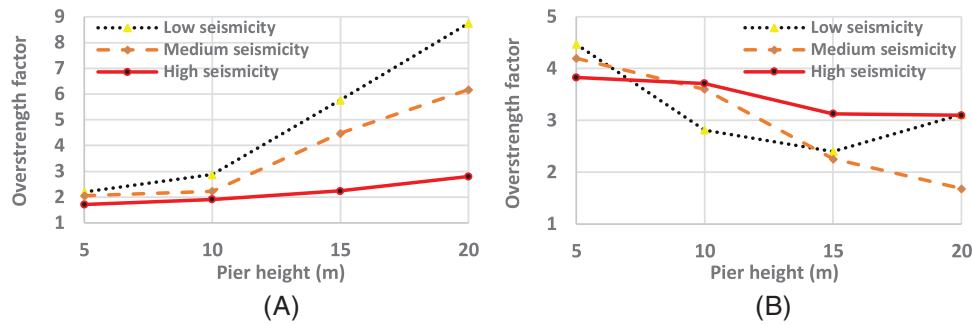


FIGURE 13 Overstrength factors of 50 m span bridges with substructure composed of multi-column piers. (A) Longitudinal direction and (B) transverse direction

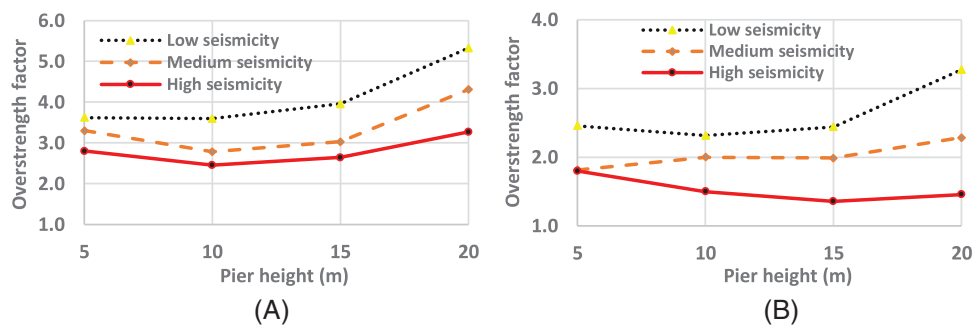


FIGURE 14 Overstrength factors of 50 m span bridges with substructure consisted of single column piers. (A) Longitudinal direction and (B) transverse direction

bridges with piers heights of 5 and 20 m, which are also the bridges with more and less impact of gravitational loads in the design of the structures.

Again, there are remarkable differences in the overstrength factors in both translational directions of the bridges due to the cantilever lateral deformation of piers and the abutment contribution in the longitudinal direction, and the frame-type configuration in the transverse direction. Similarly to the results of the 30 m span bridges, the influence of the seismic location of the bridges on the overstrength factors relates to the different impact that gravity loads had in the design actions, which is greater in the zones of lower seismicity, an effect also described by Jain and Navin.<sup>15</sup>

Figure 14 shows the overstrength factors of the 50 m span bridges supported on single column piers. The figure on the left (14a) corresponds to the longitudinal direction of the bridges and the figure on the right (14b) to the transverse direction. In both directions of analysis, up to 10 or 15 m pier height, the overstrength factor decreases as the bridges' height increases.

The overstrength factors in the longitudinal direction were in the range of 3.6–5.3, 2.8–4.3, and 2.5–3.3 for the low, medium and high seismicity zones. These values were close to those obtained for 30 m span bridges. In the transverse direction (Figure 14B), the computed overstrength factors were in the range of 2.3–3.3, 1.8–2.3, and 1.4–1.8 from low to high seismicity zones. These values were also comparable to the overstrength factors found in the transverse direction of 30 m span bridges supported on single-column piers.

Conversely, 30 and 50 m span bridges with substructure formed by single column piers, presented behavior differences in the longitudinal and the transverse directions. In the longitudinal direction, abutments had participation on the seismic response of the bridges, whereas this contribution was negligible in the transverse direction.

Despite the previous results, the influence of span length on overstrength factors was practically negligible. This is clearly observed when plotting the overstrength factors as a function of the normalized variable  $T(H/L)$  shown in the next section.

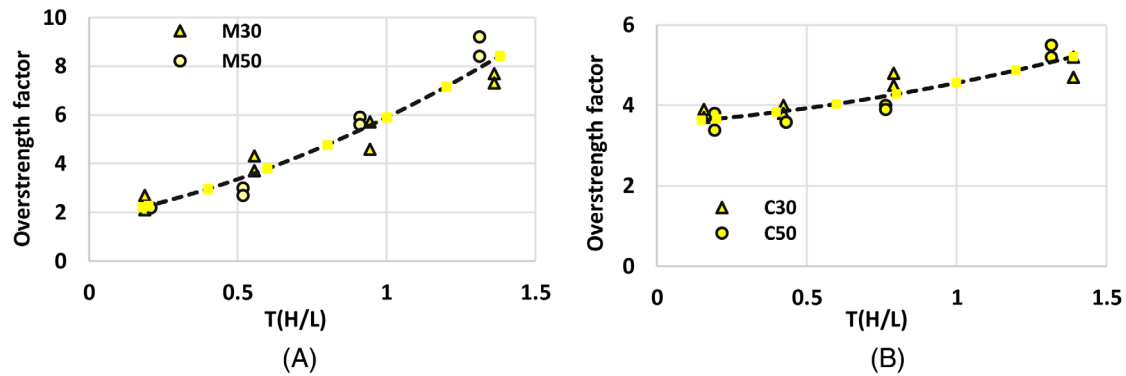


FIGURE 15 Overstrength functions in the longitudinal direction of the bridges located in the low seismicity zone. (A) Multi-column piers (M models) and (B) single column piers (C models)

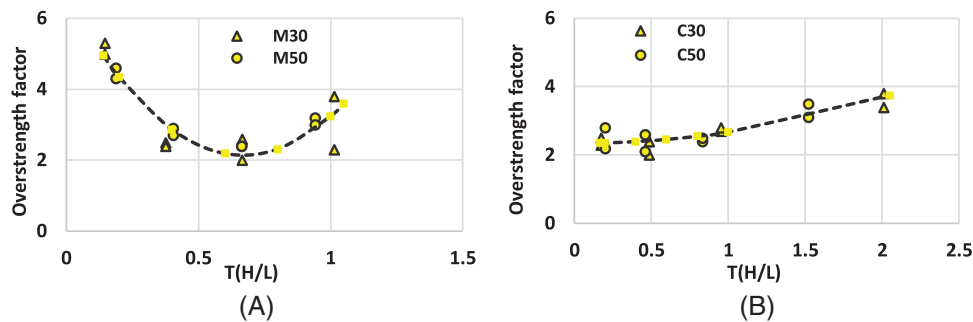


FIGURE 16 Overstrength functions in the transverse direction of the bridges located in the low seismicity zone. (A) Multi-column piers (M models) and (B) single column piers (C models)

## 6 | OVERSTRENGTH FUNCTIONS

Based on the results of the non-linear dynamic analyzes of 48 numerical models of bridges subjected to a set of 80 accelerograms recorded in Mexico, polynomial equations are proposed to evaluate the overstrength factors of the bridges. Figure 15 shows the overstrength factors in the longitudinal direction of the bridges located in the low seismicity zone. The vertical axis presents the overstrength factor and the horizontal axis displays the ratio  $T(H/L)$ .  $T$  is the fundamental period of the bridge in the direction of analysis;  $H$  is the pier height and  $L$  is the span length. Graphing the overstrength factors as a function of  $T(H/L)$  allows showing the results of both models (M30 and M50 or C30 and C50) in the same figure. Figure 15 also shows the polynomial curve fitted to the data. Figure 15A displays the results of the multi-column bridges and Figure 15B presents the results of the bridges supported on single column piers. The growth of the overstrength factor with the increase of the parameter  $T(H/L)$  is more important for bridges with multi-column piers, as compared with the bridges on single column piers.

Figure 16 shows the overstrength factors in the transverse direction of the bridges located in the low seismicity zone. Again, the change of the overstrength factors with the increase of  $T(H/L)$  was smaller in bridges supported on single column piers (Figure 16B) than the values obtained for bridges with a substructure composed of multi-column piers (Figure 16A). In the transverse direction, the substructure type modified more the period interval of the bridges and therefore the parameter  $T(H/L)$ .

Figure 17 shows the results to assess the overstrength factors in the longitudinal direction of the bridges located in the medium seismicity zone. In general, the overstrength factor decreases when passing from the low to medium seismicity zone and the highest overstrength factor was obtained for the highest value of  $T(H/L)$  in both types of substructure (Figures 17A and 17B).

Figure 18 shows the overstrength factors in the transverse direction of the bridges located in the medium seismicity zone. The overstrength factors of frame-type substructures (Figure 18A), decrease when increasing the parameter  $T(H/L)$ . On the contrary, bridges with single-column piers (Figure 18B) increase the overstrength factor with this parameter.



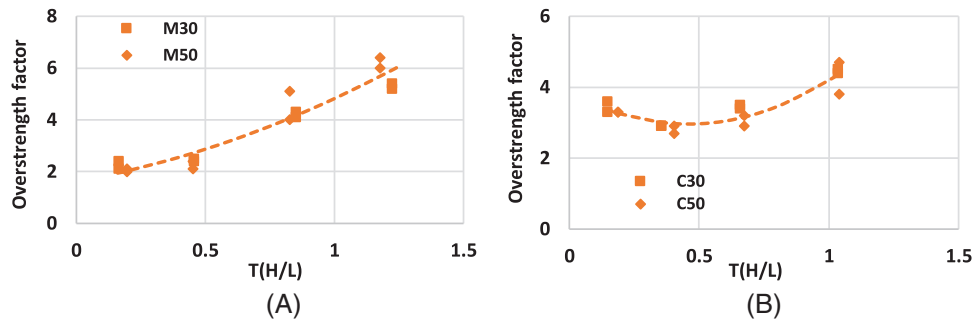


FIGURE 17 Overstrength functions in the longitudinal direction of the bridges located in the medium seismicity zone. (A) Multi-column piers (M models) and (B) single column piers (C models)

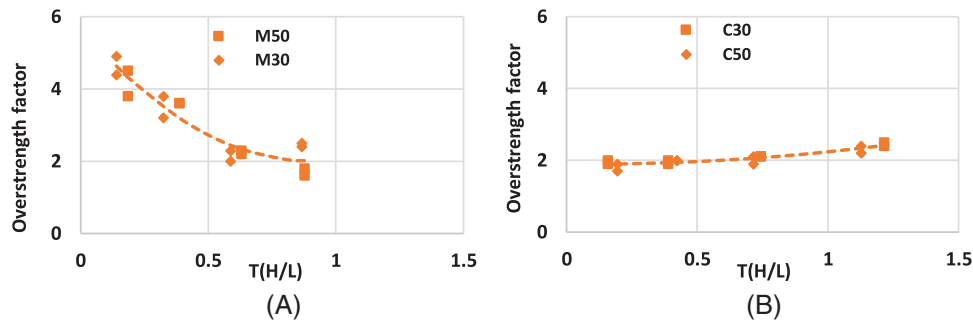


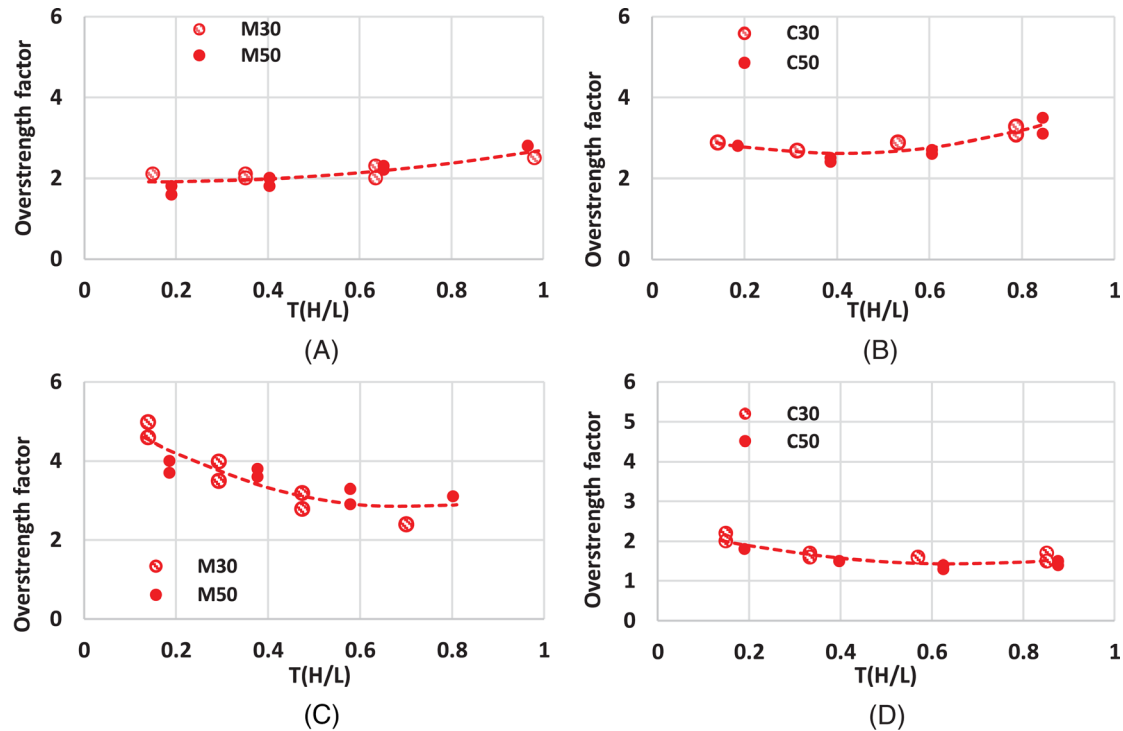
FIGURE 18 Overstrength functions in the transverse direction of the bridges located in the medium seismicity zone. (A) Multi-column piers (M models) and (B) single column piers (C models)

Figure 19 shows four graphs of the overstrength factors in both directions of analysis for bridges located in the high seismicity zone (Figures 19A and 19B in the longitudinal direction and Figures 19C and 19D in the transverse direction). The importance of the fundamental periods of the bridges in the overstrength decreases when they were in the high seismicity zone. However, even in this seismic zone, the direction of analysis was relevant in the trend and values of the overstrength factors, including the case of substructures formed by single column piers. Again, the bridges supported on single column piers had larger overstrength factors in the longitudinal direction (Figure 19B) than the factors in the transverse direction (Figure 19D) because the bridge abutments modify the seismic behavior in the former case.

As observed in previous section, the different influence of the period on the overstrength factors of the bridges located in the low seismicity zone with respect to the high seismicity zone, is mainly because gravitational loads had larger impact on pier dimensions and reinforcement in low seismicity zone than for high seismicity areas. The increase of the fundamental period also reduces the seismic demands leading to lower design base shear. Additionally, the increase of the bridges' fundamental period when passing from the lowest to the tallest piers is greater in the lower seismicity area than in the higher seismicity area, and the design spectra have decreasing demands from the period  $T_b = 0.6$  in both seismic zones.

The seismic design of bridges worldwide often incorporates reduction factors that are function of different parameters. The  $R$  factors that are applied to reduce the design spectra in the AASHTO code standard depend on the importance of the bridges classified as: Critical, Essential, and Other. For bridges with a single column substructure the  $R$  factors are in the range 1.5–3.0, whereas the factors for substructures composed of multi column bents are in the range 1.5–5.0. Eurocode 8 specifies reduction factors  $q$  in the range 1.5–3.5 as a function of the substructure ductile capacity. Sánchez-Ricart<sup>32</sup> showed reduction factors used in seismic codes for 27 countries, which are in the range 2.0–12. The great diversity among reduction factors that also makes unviable to compare directly one with the other, is related to: different methodologies used to obtain the design spectra in each country; different return periods ( $T_r$ ) used to define the design earthquake (e.g., AASHTO code  $T_r = 1000$  years, Eurocode 8:  $T_r = 475$  years, and variable  $T_r$  in Mexico throughout the country); different ratios of gravity/seismic load in each country; different characteristics of the earthquake-generating processes in each site, among others.

However, the trends of overstrength factors observed in this study are similar to those recommended in seismic codes of other countries. For example, 30 m span bridges with a substructure formed by a single column presented overstrength



**FIGURE 19** Overstrength functions of the bridges supported in multi-column piers (M models) and single column piers (C models) located in the high seismicity zone. (A) M30 and M50 in the longitudinal direction; (B) C30 and C50 in the longitudinal direction; (C) M30 and M50 in the transverse direction and (D) C30 and C50 in the transverse direction

factors in the range of 1.6–4.9 and the bridges composed of multi-column piers had overstrength factors in the range of 2.1–7.5. The lowest reduction factors recommended in the AASHTO standards (1.5) are independent of the type of substructure (in this study the lowest values obtained for single and multi-column piers were 1.6 and 2.1, respectively). Moreover, the ratio of the maximum reduction factor of multi-column piers to single-column piers in AASHTO standards is  $5/3 = 1.67$ , whereas this ratio was  $7.5/4.9 = 1.53$  in this study.

Finally, Table 3 shows the overstrength functions obtained in three seismic zones for RC bridges supported on multi-column and single column piers. The overstrength factors depend on the fundamental period ( $T$ ), pier height ( $H$ ), and span length ( $L$ ).

The above equations aim at quantifying the overstrength factors of simply supported reinforced concrete bridges with 30 and 50 m spans lengths. The main objective of this study was to show the impact of the fundamental period, the seismic zone, the piers height and the span length on the bridge overstrength. For a seismic code, it would be advisable to reduce the number of parameters by grouping the results into two or three more general classifications, a task that is beyond the scope of this study.

## 7 | CONCLUSIONS

This study determines analytical expressions to evaluate overstrength factors in RC bridges with a superstructure formed by RC slab and simple-supported prestressed concrete girders. Two types of substructures were analyzed: the first one composed of multi-column piers and the second one formed by single column piers. The bridge typologies considered five-span bridges with span lengths of 30 and 50 m. To assess the overstrength factors, non-linear dynamic analyzes were performed, subjecting the bridges to a set of 80 accelerograms recorded in the Mexican Republic.

The ratio of the ultimate base shear of the bridges divided by the design base shear determined the overstrength factors. The evaluation of the ultimate base shear assumed that there is no premature failure in the bridge before reaching the pier capacity.

The seismic zone has an important influence on the overstrength factors in the longitudinal direction of bridges supported in multi-column bents. When seismic forces have the major contribution to the design actions, the overstrength

TABLE 3 Overstrength functions for RC bridges supported on multi-column and single column piers

Bridge pier	Direction	Seismic intensity zone	Overstrength function
Multi-column	Longitudinal	Low	$q_s = 1.78 \left( \frac{TH}{L} \right)^2 + 2.41 \left( \frac{TH}{L} \right) + 1.71$
		Medium	$q_s = 1.42 \left( \frac{TH}{L} \right)^2 + 1.78 \left( \frac{TH}{L} \right) + 1.62$
		High	$q_s = 1.09 \left( \frac{TH}{L} \right)^2 - 0.33 \left( \frac{TH}{L} \right) + 1.94$
	Transverse	Low	$q_s = 10.03 \left( \frac{TH}{L} \right)^2 - 13.42 \left( \frac{TH}{L} \right) + 6.63$
		Medium	$q_s = 4.66 \left( \frac{TH}{L} \right)^2 - 8.28 \left( \frac{TH}{L} \right) + 5.70$
		High	$q_s = 5.38 \left( \frac{TH}{L} \right)^2 - 7.57 \left( \frac{TH}{L} \right) + 5.49$
Single-column	Longitudinal	Low	$q_s = 0.46 \left( \frac{TH}{L} \right)^2 + 0.56 \left( \frac{TH}{L} \right) + 3.53$
		Medium	$q_s = 4.22 \left( \frac{TH}{L} \right)^2 - 3.87 \left( \frac{TH}{L} \right) + 3.85$
		High	$q_s = 3.69 \left( \frac{TH}{L} \right)^2 - 3.00 \left( \frac{TH}{L} \right) + 3.23$
	Transverse	Low	$q_s = 0.34 \left( \frac{TH}{L} \right)^2 - 0.018 \left( \frac{TH}{L} \right) + 2.34$
		Medium	$q_s = 0.40 \left( \frac{TH}{L} \right)^2 - 0.052 \left( \frac{TH}{L} \right) + 1.89$
		High	$q_s = 2.21 \left( \frac{TH}{L} \right)^2 - 2.89 \left( \frac{TH}{L} \right) + 2.37$

factors showed less dependence on the pier's height, which occurs in high seismicity zones. The foregoing is understandable when observing that the ultimate base shear increases in a similar way to the design shear in high seismicity zones. However, when the gravity load is relevant in the design actions, as occurs in low seismicity zones, the ultimate base shear increases whereas the design base shear reduces with the increment of pier length increasing the overstrength factors. The same attenuated effect occurs in both directions of bridges supported by single-column piers, where, as expected, the fewer columns the pier has (less redundant), the lower the overstrength factors.

The overstrength factors were also greater in the longitudinal direction than in the transverse direction, as a result of the soil-abutment contribution to the bridge capacity. The increase of the longitudinal displacement demands (taller piers) enlarge the abutment participation. The effect of abutments is also shown in single column piers where the overstrength factors are greater in the longitudinal direction than in the transverse direction.

In the transverse direction of the bridges supported in multi-column bents, the trends are different from the longitudinal direction in view of the pier lateral deformation in double curvature. The important contribution of gravitational loads on the design actions for low-height bridges led to high overstrength values that decreased as the bridge height increases where there is greater influence of seismic demands in the design actions. Additionally, the low stiffness of the 20 m high piers led to collapse damage state for lower shear forces than those of the 5 m high bridges. Moreover, the fundamental periods in the transverse direction of the bridges were shorter than in the longitudinal direction which, according to the response and design spectra, increase the seismic demands and consequently reduce overstrength factors.

The dependence of the overstrength functions for simply-supported bridges on the participation ratio of gravity to seismic loads in the design actions is relevant in Mexico where truck loads are particularly different from trucks used to design bridges in other countries. This study initiates the first efforts towards including overstrength factors for bridges in Mexican code-standards, supported by analytical studies. The selection of these factors should also incorporate a deeply review of the values suggested by other authors and bridge code-standards in the world. An additional study should explore to use a narrow variation of overstrength factors in the longitudinal and transverse directions, which could be carried out in the future works aiming at proposing specific values to be adopted in Mexico bridge code-standards.

The results also showed that the overstrength factors in both directions of analysis depended very marginally on the bridges' span. This was evident by observing the overstrength factors of 30 and 50 m span bridges with height variation in the range of 5–20 m, as a function of the variable  $T(H/L)$ ,  $T$  = fundamental period (s),  $H$  = pier height (m), and  $L$  = span length (m).

The applicability of the proposed analytical expressions is limited to the typologies studied. The superstructure was composed of prestressed girders with a 0.20 m thick RC slab. The simply supported girders, with span lengths in the range of 30–50 m, rested on elastomeric bearings and on circular single and multi-column piers. Additionally, the bridges were designed using current Mexico code standards and assumed to be located in sites of hard soil. It would be desirable that future works consider other substructure classes and bridges supported on foundations designed for other types of soil.

## ACKNOWLEDGMENTS

The authors gratefully acknowledge the scholarship No. 259 for the first author provided by PRODEP (DSA/103.5/15/9726), and the financial support of the Universidad Michoacana de San Nicolás de Hidalgo, México. Part of this work reports to research financially supported by Project POCI-01-0145-FEDER- 007457—CONSTRUCT, Institute of R&D in Structures and Construction, funded by FEDER funds through COMPETE2020 and by national funds through Fundação para a Ciência e a Tecnologia (FCT). This work was also developed within the scope of the project proMetheus—Research Unit on Materials, Energy and Environment for Sustainability, FCT Ref. UID/05975/2020, financed by national funds through the FCT/MCTES.

## DATA AVAILABILITY STATEMENT

Research data are not shared

## ORCID

António Arêde  <https://orcid.org/0000-0002-0901-2214>

Jose M. Jara  <https://orcid.org/0000-0003-2431-017X>

Pedro Delgado  <https://orcid.org/0000-0002-4024-0442>

## REFERENCES

1. Frías AR, Disaster experiences in Bridges of México. [http://www.amivtac.org/spanelWeb/filemanager/Biblioteca\\_Amivtac/Seminario-Internacional-Puentes/SIII/SIII-Experiencias-de-Desastres-en-puentes-de-Mexico.pdf](http://www.amivtac.org/spanelWeb/filemanager/Biblioteca_Amivtac/Seminario-Internacional-Puentes/SIII/SIII-Experiencias-de-Desastres-en-puentes-de-Mexico.pdf). Accessed November 24, 2020
2. Bertero V, Hart GC, Anderson JC, et al. Design guidelines for ductility and drift limits. *Earthquake Eng Res Cent Rep*. 1991.
3. Elnashai AS, Mwafy AM. Overstrength and force reduction factors of multistorey reinforced-concrete buildings. *Struct Des Tall Spe Build*. 2002;11(5):329-351.
4. Luaces FL, *Sobrerresistencia de estructuras a base de marcos de concreto reforzado*. MSc Thesis, División de Estudios de Posgrado. Facultad de Ingeniería, Universidad Nacional Autónoma de México. México. 1995
5. Ordaz, et al. Proposal of seismic design spectra for the Federal district. *Revista Internacional de Ingeniería de Estructuras*. 2003;8(2):189-207.
6. Park R, Explicit incorporation of element and structure overstrength in the design process. Proceedings of the 11th WCEE. Acapulco, México. 1996.
7. Paulay T, Seismic design of concrete structures the present need of societies. Proceedings of the 11th World Conference on Earthquake Engineering. Acapulco, México. 1996
8. Varela J, Chan S, Fernández L. Overstrength in autoclaved aerated concrete structures. *Ingeniería*. 2008;12(2):45-55.
9. Miranda E, Bertero V. The Mexico earthquake of September 19, 1985—performance of low-rise buildings in Mexico City. *Earthq Spectra*. 1989;5(1):121-143.
10. Osteraas JD, Krawinkler H. In: John A, ed. *Strength and Ductility Considerations in Seismic Design*. Stanford, California: Blume Earthquake Engineering Center. Stanford University; 1990. Report No. 90.
11. UBC. Uniform Building Code. *Struct Eng Des Prov*. 1997.
12. Shahrooz BM, Moehle JP. Evaluation of seismic performance of reinforced concrete frames. *J Struct Eng*. 1990;116(5):1403-1422.
13. Cassis JH, Bonelli P, (1992). Lessons learned from the March 3, 1985 Chile earthquake and related research. *Proceedings of the 10th World Conference on Earthquake Engineering*. Madrid, España. 1992.
14. Zhu TJ, Tso WK, Heidebrecht AC. Seismic performance of reinforced concrete ductile moment-resisting frame buildings located in different seismic regions. *Can J Civ Eng*. 1992;19(4):688-710.
15. Jain SK, Navin R. Seismic overstrength in reinforced concrete frames. *J Struct Eng*. 1995;121(3):580-585.
16. Rahgozar MA, Humar J. Accounting for overstrength in seismic design of steel structures. *Can J Civ Eng*. 1998;25(1):1-15.
17. Balendra T, Huang X. Overstrength and ductility factors for steel frames designed according to BS 5950. *J Struct Eng*. 2003;129:1019-1035.
18. Massumi A, Tasnimi AA, Saatcioglu M, Prediction of seismic overstrength in concrete moment resisting frames using incremental static and dynamic analyses. *Proceedings of the 13th World Conference on Earthquake Engineering*. Vancouver, BC, Canada. 2004.
19. Ghee AB, Priestley MJN, Paulay T. Seismic shear strength of circular reinforced concrete columns. *J Struct*. 1989;86(1):45-59.
20. Kappos AJ, Paraskeva TS, Moschonas IF. Response modification factors for concrete bridges in Europe. *J Bridge Eng*. 2013;18(12):1328-1335.
21. MOC. Design manual of civil works. *Seismic Design*. Electrical Research Institute (IIE). 2015. México.

22. II-UNAM. *Instituto de Ingeniería de la UNAM y Universidad Nacional Autónoma de México*. Base de Datos de Registros Acelerográficos de la Red Sísmica Mexicana. México. 2017.
23. Von Thun JL, Roehm LH, Scott GA, Wilson JA. Earthquake ground motions for design analysis of dam. *Earthquake Engineering and Soil Dynamics II – Recent Advance in Ground-Motion Evaluation*. New York: ASCE; 1988:463-481. Geotechnical Special Publication 20.
24. Frias AR, Rehabilitation and retrofit of Bridges in México. *Proceedings of the 4th International Bridge Design Symposium*. 2013. Morelia, Michoacán México, 4-6 July.
25. Caltrans. Bridge design practice. *Seismic Design of Concrete Bridges*. Chapter 21. In California Department of Transportation. Sacramento, California. 2015.
26. CSI. *SAP2000, V19.2.1 Ultimate*. Computers and Structures, Inc. Berkeley, California. 2017
27. AASHTO. AASHTO LRFD Bridge Design Specifications, 8th ed. *American Association of State Highway and Transportation Officials*. Washington DC. 2017.
28. DFD District Federal Department. Technical Regulation for Seismic Design. Gaceta Oficial de la Ciudad de México, No. 220 Bis, 15 de diciembre de 2017, Ciudad de México, México (in Spanish). 2017.
29. Mander JB, Priestley MJN, Park R. Theoretical stress-strain model for confined concrete. *J Struct Eng*. 1988;114:1804-1826.
30. Park R, Paulay T. *Reinforced concrete structures*. John Wiley & Sons; 1975.
31. Paulay T, Priestley MJN. *Seismic design of reinforced concrete and masonry buildings*. John Wiley & Sons; 1992.
32. Sánchez-Ricart L. Reduction factors in seismic codes: on the components to be taken into account for design purposes. *Georisk*. 2010;4:208-229.

**How to cite this article:** Sánchez AR, Arêde A, Jara JM, Delgado P. Overstrength factors of rc bridges supported on single and multi-column rc piers in Mexico. *Earthquake Engng Struct Dyn*. 2021;1-18.  
<https://doi.org/10.1002/eqe.3528>